Structural Analysis During Creep Process of Ultrahigh-Strength Polyethylene Fiber

YASUO OHTA, ATSUSHI KAJI, HIROSHIGE SUGIYAMA, HIROSHI YASUDA

Toyobo Research Center Company, Ltd., 1-1 Katata 2-Chome, Ohtsu, Shiga 520-0292, Japan

Received 6 October 1999; accepted 5 April 2000

ABSTRACT: Structural changes during the creep process of ultrahigh-strength polyethylene fiber (UHSPE) were investigated using X-ray and the solid-state NMR techniques. As the creep strain increases, the quantity of the amorphous phase area estimated by the ^{13}C-NMR method increases until the final creep rupture. On the other hand, the amorphous quantity estimated by the X-ray method does not change noticeably. To explain this contrast, we proposed a new model that illustrates how the defects such as chain ends incorporated into the crystalline phase are excluded from the crystallite and agglomerate to generate a new amorphous area, which has a size hardly detected by the X-ray method. These small amorphous areas are considered to cause a decrease in the tensile strength and the successive final creep rupture. © 2001 John Wiley & Sons, Inc. J Appl Polym Sci 81: 312–320, 2001

Key words: ultrahigh-strength polyethylene fiber; creep; WAXD; ^{13}C-NMR

INTRODUCTION

Ultrahigh-strength polyethylene (UHSPE) fibers have been developed by the gel-spinning method.[1–3] Although the fibers possess extremely high strength and modulus, their creep-resistance property is inferior to other high-strength fibers such as Aramid fiber, which has a rigid molecular structure. This inferior creep property is derived mainly from the simple chemical structure of polyethylene, which has no strong interaction among molecular chains such as a hydrogen bonding.

Numerous studies on the creep process of polyethylene have been made.[4–16] However, most of this attention focused on the rheological analyses of creep deformation and not on the structural changes during the creep process. One reason for this comes from the situation that a conventional polyethylene material such as a melt-crystallized one has a very complicated microstructure composed of crystalline and amorphous phases. On the other hand, UHSPE fiber is known to posses a highly oriented molecular structure within an almost 100% crystallinity. Therefore, the UHSPE fiber sample can be regarded as an ideal material for a structural study, especially focusing on the crystalline-deformation change during the creep process.

Wilding and Ward[14–16] reported the creep properties of UHSPE fibers in detail. They concluded that the mechanism of the creep phenomena of UHSPE fibers at relatively high creep stress (ca. $>$0.2 GPa) is similar to that for the α-relaxation process of the dynamic viscoelastic properties, meaning that the chain slippage occurs at the interface such as an intracrystallite (chain-to-chain slip) and/or an intercrystallite (grain boundary slip) in the crystalline during the creep process. In our previous studies,[17,18] we found that the creep process of UHSPE fibers at a relatively high stress condition is dominated

Correspondence to: Y. Ohta.

Journal of Applied Polymer Science, Vol. 81, 312–320 (2001)

mainly by intracrystallite (chain-to-chain) slippage rather than intercrystallite (grain boundary) slippage. If such intracrystallite chain slippage proceeds as a steady creep deformation, it should be difficult to detect an apparent structural change. Indeed, the creep strain rate of the tested UHSPE fiber is almost constant within the experimental time range as described later, meaning that the creep deformation proceeds as a steady-flow deformation. On the other hand, a sudden yarn breakage is also observed after this steady-flow deformation, implying that some structural fatigue or destruction is accumulating prior to the final yarn breakage during the steady-flow deformation period. Therefore, a detailed study on structural changing during the creep process will be worthwhile in understanding the nature of the creep and the creep rupture of UHSPE fibers. In this article, using ^{13}C-NMR,[19–22] X-ray, and other methods, the structural changes during the creep process of UHSPE fibers were investigated. In addition, the relationship between structural and mechanical property changes during the creep process are discussed.

EXPERIMENTAL

Sample Preparation

UHSPE fibers were prepared by the gel-spinning method.[1–3] A commercial-grade UHMW-PE (Hizex240M, $M_w = 3.0 \times 10^6$ g/mol, $M_w/M_n \sim 12$) by Mitsui Chemical (Japan) was used in this study. Five weight percent of the polymer was dissolved with 95 wt % decalin (deca-hydronaphthalene) with an antioxidant agent (BHT, 2,6-*tert*-butyl-*p*-cresol) of 1 wt % of the polymer at 200°C by a screw-type mixer. Gel fibers (solvent containing gel-like fibers) spun at a throughput of 1 g/min through a spinneret having a diameter of 0.8 mm at 160°C were subsequently cooled by nitrogen gas at room temperature under a stretching deformation with a take-up speed of 50 m/min. The solvent-contained gel fibers were subsequently drawn at a draw ratio of 5 at 100°C in an air oven. These obtained fibers were again drawn at the draw ratio of 4 at 145°C.

Creep Measurement and Sample Preparation

Creep measurements were conducted in an air oven adjusted to the temperature of 70°C, and a creep stress of 0.52 GPa (20% of the breaking stress of the initial fiber) was applied. The temperature was controlled within 2°, and a pretension of 0.1 g/d was applied for the sample setting. After the temperature of the sample become stable, the testing creep stress was loaded and then the strain was recorded. The creep-deformed samples, which experienced different creep strain histories, were obtained by removing the creep stress after a certain different elapsed time for each sample.

Tensile Testing

Tensile testing was carried out on a Tensilon™ tensile tester (Orientec Co., Ltd.) at 25°C and at a strain rate of 1 min^{-1} with an initial sample length of 100 mm. The typical mechanical properties of the representative samples obtained with this method are listed in Table I.

X-ray Analysis

A crystallite size, an orientation factor of the crystalline, and a unit cell size were determined using wide-angle X-ray diffraction (WAXD) for each sample after the creep stress was removed. Each sample was wound on a metal holder carefully so that filaments were aligned to each other until enough thickness for the scattering intensity could be obtained.

WAXD experiments were carried out on a Rota RA™ (Rigaku Co., Ltd.) using Ni-filtered CuKα radiation at a filament power of 50 kV and 100 mmA. Unit cell sizes of the a- and b-axes of an orthorhombic system were determined using peak positions of (110) and (200) diffraction. The house-made peak separation program was applied to the obtained diffraction pattern. By using the Gaussian curve, the fitting was successfully conducted. By using each separated peak, the paracrystallinity (the second-order imperfection) of the crystallite (g_2) and their size (L_{hkl}) was

Table I Tensile Properties of Ultra-High Strength Polyethylene Fibers Subjected to Different Creep Deformation

Creep Strain (%)	Tensile Strength (GPa)	Tensile Modulus (GPa)
0	2.6 ± 0.1	95 ± 2
2.0	2.7 ± 0.1	106 ± 2
4.0	2.4 ± 0.1	93 ± 2
6.0	2.2 ± 0.2	85 ± 2

determined by using the Hosemann method for Gaussian-curve-type fitting,[23] which can be described by the following equation:

$$(\delta s)^2_{\exp} = \frac{1}{\bar{L}^2_{hkl}} + \frac{(\pi g_2)^4 m^4}{\bar{d}^2_{hkl}} \quad (1)$$

where δs is the integral breadth of each diffraction pattern of successive planes (hkl) in series, for example, (110), (220), and (330). L_{hkl} is the crystalline size; d_{hkl}, the spacing of the plane (hkl) of the unit cell; g_2, the parameter of distortions of the second kinds, and m, the order number for each peak.

For the Hosemann method, at least three peaks in series [e.g., (110), (220), and (330)] are necessary. However, in the case of UHSPE fibers, especially for the highly drawn sample used in this study, the linear fitting with three successive peaks was sometimes difficult. Although the reason for this is unclear (maybe due to some structural characteristic of the UHSPE fiber), we tried to use the first two peaks conventionally, that is, (110), (220) and (200), (400), for the g_2-value determination in this study. Each peak width was corrected by considering the effect of the slitting beam size and other geometrical effects.

The crystalline orientation factor (f_c) was calculated with eq. (2):

$$f_c = (180 - W_{110})/180 \quad (2)$$

where W_{110} (degree) is the width at half-height of the diffraction peak obtained by scanning in the meridian direction for (110) diffraction.

Finally, by using the decomposed peak height, the amount of amorphous area and also the monoclinic crystalline area were conventionally determined. This will be described again below.

^{13}C-NMR Experiment

Solid-state high-resolution ^{13}C-NMR spectra were measured using a Varian XL-300 (^{13}C, 75.5 MHz) at ambient temperature. Dipole decoupling power was about 50 kHz. Fine-tuning of the spectrometer was conducted to obtain sufficiently narrow line widths. The magic angle spinning rate was about 3.5 kHz. Other detailed procedure including the pulse sequence is described in the previous article.[19]

^{13}C-NMR spectra were divided into three several Lorentzians by the least-squares method, each of which corresponds to the orthorhombic phase (ORC) at 33 ppm, the monoclinic phase (MCC) at about 34.3 ppm, and the amorphous phase at 31.2 ppm. The basis of the identification of each peak was also described in detail previously.[19] We tried to estimate the crystallinity, that is, the crystalline and amorphous ratio, by using the peak height ratios from each phase. All experiments were conducted with the cross polarization time, T_{cp}, of 1 ms.

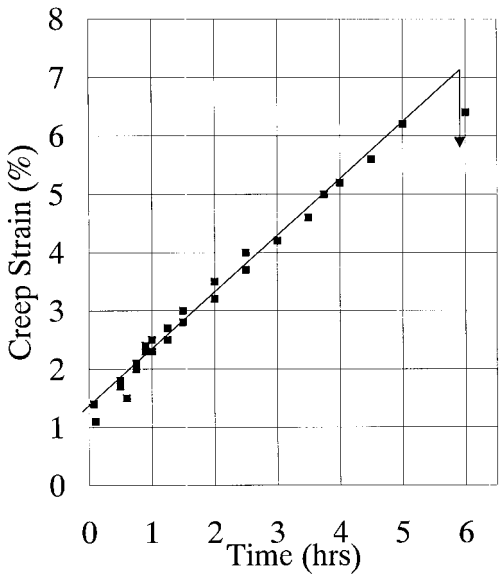

Figure 1 Creep-deformation curve obtained at the temperature of 70°C and the loading creep stress of 0.52 GPa.

RESULTS AND DISCUSSION

Creep Properties

A typical creep strain curve obtained at 70°C and the creep stress of 0.52 GPa (20% of the initial tensile strength) is plotted against time in Figure 1. As already mentioned, it should be noted that the creep deformation of the UHSPE fiber proceeds as the steady-flow deformation until the sudden creep rupture occurs. An apparent increase in the creep rate prior to the creep rupture was not observed, which is normally observed for other material.

It has been reported that the creep deformation of UHSPE fiber can be described with a simple viscoelastic function, namely, the creep strain λ can be expressed by a superposition of three dif-

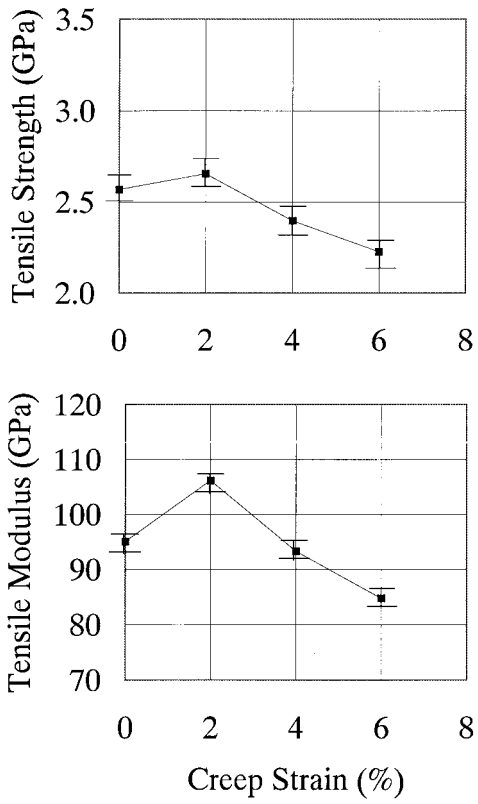

Figure 2 Tensile strength and modulus versus creep strain (70°C, 0.52 GPa) measured at room temperature and after creep stress removal.

ferent strain components as shown with following equation:[14–16]

$$\lambda = \lambda_1 + \lambda_2 + \lambda_3 \tag{3}$$

where λ_1 is identified as an "elastic component" which is constant with elapsed time and proportional to a subjected stress. λ_2 is identified as a "delayed elastic component" which increases with the elapsed time and also approaches to a constant value in relatively short time range. Finally λ_3 is identified as a "viscous component" which increases linearly with time (t) as follows:

$$\lambda_3 = \dot{\varepsilon}_p \times t \tag{4}$$

$$\dot{\varepsilon}_p = \dot{\varepsilon}_0 \exp(-\Delta H/kT)\sinh(\sigma v/kT) \tag{5}$$

where $\dot{\varepsilon}_p$ is the creep rate; $\dot{\varepsilon}_0$, a material constant; ΔH, the activation energy; v, the activation volume; σ, the applied stress; T, the temperature; and k, the Bolzmann constant.

Apparently, λ_3 is regarded to be the dominant component. In other words, the creep deformation of the UHSPE fiber can be simply described as the viscous deformation or the steady-state flow deformation. In previous articles,[17,18] we reported that the creep process of UHSPE fibers is dominated mainly by the molecular deformation in the crystalline part, namely, the chain slippage occurs within the crystalline phase, whose molecular motion is analogous to that of the α2-relaxation process (intracrystallite relaxation) of polyethylene. Therefore, if the creep process proceeds as a steady-state deformation such as the continuous chain slippage, the obvious structural deformation and/or destruction will be hardly observed. On the contrary, the sudden creep rupture occurs at the end of the steady creep deformation. This implies that some kind of fatigue or defects should be stored and/or accumulated within the fiber structure during the steady-state process. In this study, by applying several structural-analyzing methods, we wanted to clarify the existence of the structural change during the creep deformation of UHSPE fibers.

Tensile Properties

The tensile properties of each sample having different creep strain history are also listed in Table I. Figure 2 shows the tensile properties as a function of the creep strain. It can be found that both the tensile strength and modulus increase slightly in the initial stage and successively decrease with the creep strain. This initial slight increase in the tensile properties may be attributed to the increase in the molecular orientation or a macroscopic improvement of the fiber orientation, such as the arrangement of individual filaments within the fiber bundle due to the applied stress. Figure 3 shows the change of the crystalline orientation factor f_c as a function of the creep strain. The slight increase of the f_c value in the initial stage was observed, and this result may correspond to the above hypothesis. However, the decrease in the tensile properties for the later region is unable to be explained merely with f_c.

Smook et al.[24] reported that the tensile strength of UHSPE fibers can be well described with the Griffith-type equation as follows:

$$\sigma^{-1} = K(D - D_0)^{1/2} + \sigma_0^{-1} \tag{6}$$

where σ is the tensile strength, and σ_0, the strength of a flawless fiber, which is reported

experimentally to be 26 GPa for the highly oriented UHSPE fibers by Smook et al.[24] and theoretically to be 25 GPa.[25] D is the fiber diameter and D_0 is the diameter of flawless fiber (single molecular chain), which can be practically taken as zero, and K is the material constant, which is formulated to

$$K = b(1/G_{IC}E)^{1/2} \tag{7}$$

where G_{IC} is the energy needed for the creation of a crack of critical dimensions; E, the fiber modulus; and b, the material constant.

In the creep process, the change of the fiber diameter is almost negligible; then, eq. (6) can be transformed to

$$b(D/G_{IC})^{1/2} = (\sigma^{-1} - \sigma_0^{-1})E^{1/2} \tag{8}$$

As a total, the left-side term of eq. (8) becomes the material constant, which will provide information of the degree of defect propagation within the fiber structure. This can be understood with the situation that the fiber with a higher $b(D/G_{IC})^{1/2}$ value should exhibit a lower tensile strength even though the fiber possesses the same modulus value.

Figure 4 shows $(\sigma^{-1} - \sigma_0^{-1})E^{1/2}$ as a function of the creep strain. It was found that the $(\sigma^{-1} - \sigma_0^{-1})E^{1/2}$ value monotonously increases with the creep strain. This result suggests that an accumulation of some kind of defects within the fiber structure may occur during the steady creep process. In another words, this defect-accumulation process may be the cause for the decrease in the tensile properties in higher creep strain region. In the following section, we try to clarify the structure of the defects that should correspond to the decrease in the tensile properties.

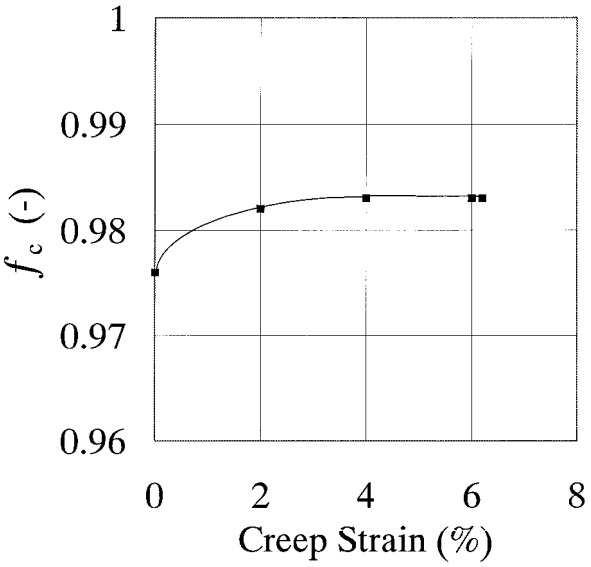

Figure 3 Orientation factor evaluated by X-ray versus creep strain.

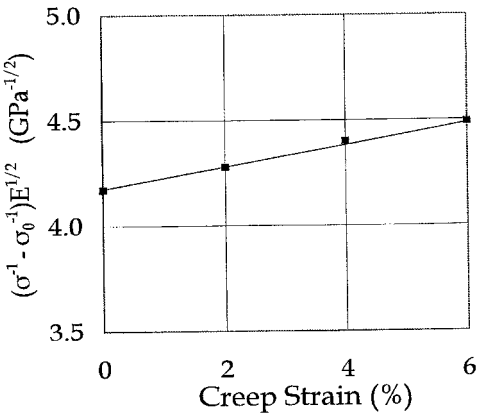

Figure 4 Defect index defined with $(\sigma^{-1} - \sigma_0^{-1})E^{1/2}$ derived from the tensile strength (σ) and modulus (E) demonstrated in Figure 3 versus creep strain; σ_0 is the theoretical strength of a flawless fiber (26 GPa).

WAXD Analysis

Figure 5 shows the typical WAXD profile of UHSPE fiber and the result of the peak separation. From each separated peak, the unit cell dimension, crystalline size, and g_2 value were determined. Figure 6 shows the unit cell dimension changes in both the a- and b-axes of an orthorhombic system as a function of creep strain. The a-axis seems to decrease slightly, while the b-axis is constant. It is unclear whether this result is significant or not. However, it is well known that the a-axis of polyethylene is more sensitive to the crystalline condition than is the b-axis. For example, incorporation of the short branches within the crystallite expands the a-axis.[26] As described later in detail, if some kind of defects such as molecular chain ends, kinks, or entanglements are excluded from the crystallite during the creep process, the a-axis should decrease with the creep strain, because such the defects have a larger excluded volume than that for the ethylene unit.

Figures 7 and 8 show the crystalline size and g_2-value changes, respectively, obtained with the peaks series both of (110) (220) and (200) (400) as a function of the creep strain. As shown in Figure

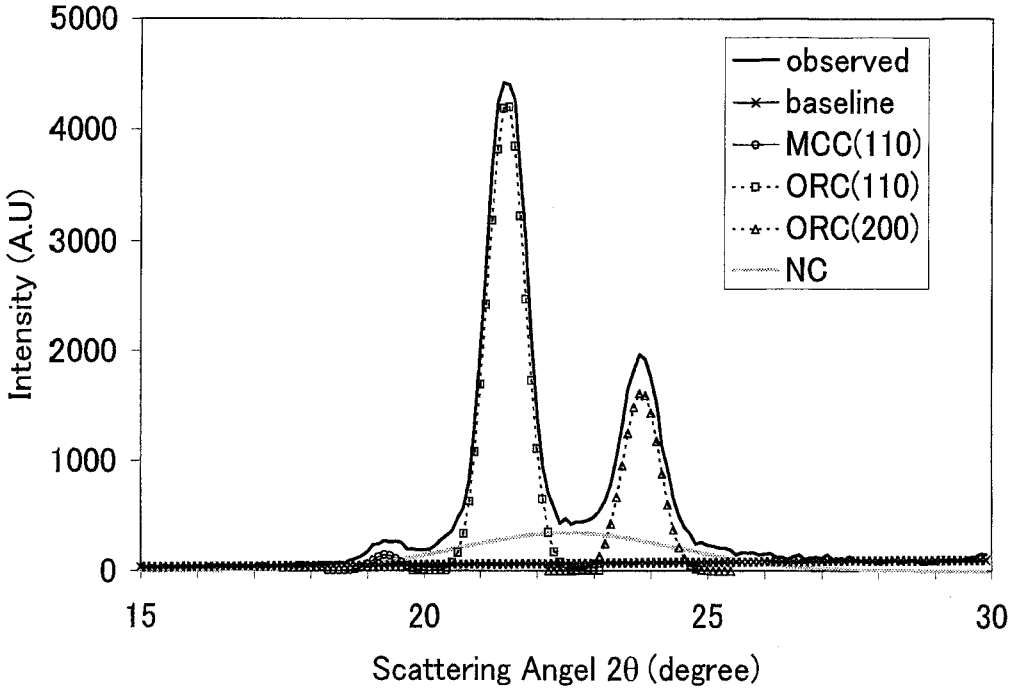

Figure 5 Typical WAXD pattern and peak-separation results for UHSPE fiber. The solid line is the observed diffraction profile and the broken lines are the peak-separation results.

7, the crystalline sizes show no obvious change with the creep strain, meaning that destruction in a large size such as the deformation of crystalline itself does not occur.

Figure 8 demonstrates that $g_2(110)$ tends to increase slightly, but no obvious trend with $g_2(200)$ was found with much larger data scattering than that of $g_2(110)$. If this trend of $g_2(110)$ is significant, it can be regarded that the second-order imperfection of crystallite, at least in the plane direction of (110), proceeds with the creep strain.

From these results, it can be concluded that not so obvious changes in the crystalline and the unit cell sizes occur up to the final creep rupture, while the a-axis size and the second-kinds imperfection of the crystalline in the direction of (110) seem to have chances to change with the creep deformation. In the next section, by using the ^{13}C-NMR technique, we try to study more detailed structure change, because the ^{13}C-NMR technique can be regarded to be sensitive to more localized molecular motion and/or phase structure information than WAXD technique.

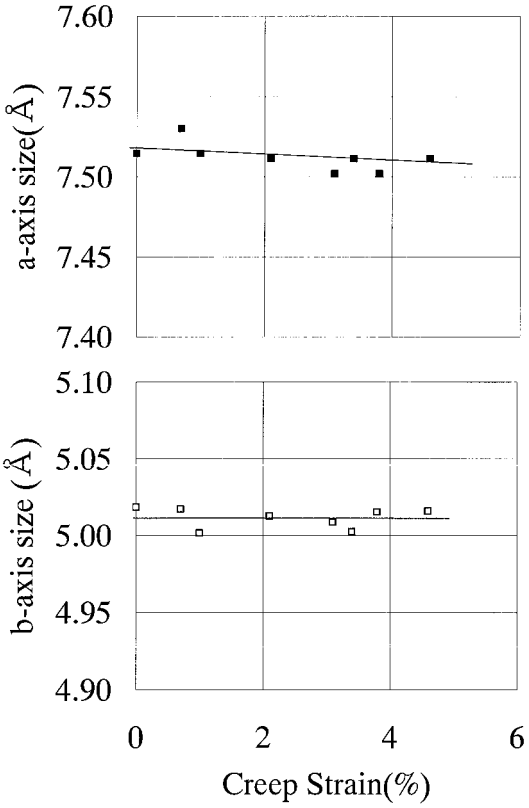

Figure 6 Axis size [(■) a-axis; (□) b-axis] of an orthorhombic crystalline system versus creep strain.

^{13}C-NMR Analysis

Figure 9 shows the typical ^{13}C-NMR spectrum obtained with the initial sample. In this figure,

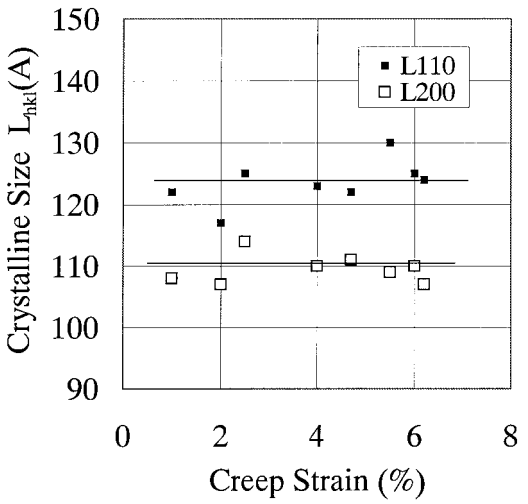

Figure 7 Crystalline size [(■) (110) direction; (□) (200) direction] evaluated by the Hosemann method as a function of creep strain.

each separated peak can be assigned to the orthorhombic crystalline phase (ORC) with the peak position at 33 ppm, the monoclinic crystalline phase (MCC) at 34.3 ppm, the amorphous phase (NC) phase at 31.2 ppm, and the intermediate phase around 33.5 ppm, separated by Lorentzians curve fitting. Using these separated spectra, the fraction of each phase, for example, the MCC-to-ORC ratio (MCC/ORC) and the NC-to-ORC ratio (NC/ORC), were determined conventionally by using each peak height. This detailed procedure was given in a previous article.[19]

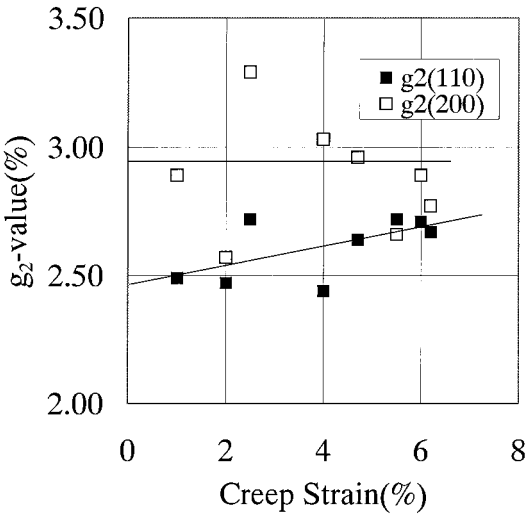

Figure 8 Paracrystallinity index (g_2 value) versus creep strain (■) for the (110) direction and (□) for the (200) direction.

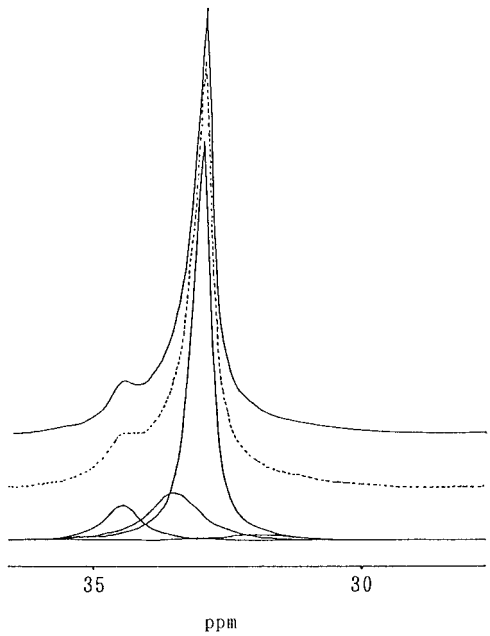

Figure 9 Typical ^{13}C-NMR spectra from ultrahigh-strength polyethylene fiber. The top solid line indicates the full spectrum, the bottom solid lines denote separated peaks for monoclinic, intermediate, orthorhombic, and amorphous phases from the low-frequency side, respectively, and the middle broken line denotes the superposition of the separated four spectra.

Table II summarizes the ^{13}C-NMR results, and in Figure 10, the variation of each phase fraction, that is, MCC/ORC and NC/ORC, is plotted against the creep strain. It was found that NC/ORC increases almost linearly with the creep strain, while MCC/ORC is almost constant. This change in the NC/ORC ratio suggests that some portion of the ORC transforms to NC monotonously as the creep propagation.

Figure 11 shows a similar evaluation using the peak heights of the WAXD patterns. In this case, no obvious change in NC/ORC was found. This discrepancy can be regarded to come from the

Table II The Results with ^{13}C-NMR Measurements

Creep Strain (%)	ORC Peak Width (Hz)	MCC/ORC (-)	NC/ORC (-)
0	33.5	0.016	0.033
2.0	31.9	0.015	0.040
4.0	31.4	0.018	0.043
6.0	32.2	0.013	0.047
6.2	35.5	0.019	0.053

difference in the size and/or the spatial length relating to the obtainable information both by the WAXD and the ^{13}C-NMR techniques. Namely, the ^{13}C-NMR technique is thought to be sensitive to relatively local molecular motion. Therefore, it can be considered that the size of the increasing amorphous potion detected by the ^{13}C-NMR technique should be a localized phenomenon which is hardly detected by the WAXD analysis. Although the existence and the origin of such a newly generating "pseudo"-amorphous area is speculative, the chain ends or molecular entanglement parts which are excluded from ORC will be the candidates for such localized small defects, namely, these small amorphous area or microvoids can regarded to be effective to decrease the tensile properties, and this result also seems to agree well with the a-axis behavior as mentioned in the WAXD section.

Molecular Mechanism

The molecular motion of the defects-exclusion process from the crystallite can be described as a dislocation process in the crystallite area such as proposed by Mansfield and Boyd.[27] In our previous reports,[17,18] we concluded that the creep mechanism of UHSPE fibers is dominated mainly by the chain slippage within the crystallite, in which defects such as the chain ends can travel in the chain direction and are finally excluded from the crystallite. This mechanism can successfully explain the tensile properties' change during the creep deformation, that is, the increase in the "pseudo"-amorphous region will induce a drop in the tensile properties, especially in the tensile strength. At the final stage of the creep process, sudden breakage is observed, implying that a catastrophic destruction of the crystalline structure or the chain breakage should occur prior to the final rupture, where the fiber cannot bear the entire loading stress. Basically, this fracture process will be understood by the mechanism of the nucleation of defects and the growth,[28] namely, the defect-nuclei (microvoids) derived from the chain ends or small defects grow into the macrovoids as reported by Prevorsek et al.[29] As mentioned previously, the ^{13}C-NMR analysis can be thought to be more sensitive to the local defects existing in the crystallite than in the WAXD analysis. The newly originated amorphous phase existing inside or nearby the crystalline phase should be very small (<10 Å), which is hardly detected by WAXD analysis. We think that these defects are mainly from the aggregation of chain ends or molecular kinks excluded from the crystallite. If the total amount of such localized amorphous areas (microvoids) exceeds the critical level

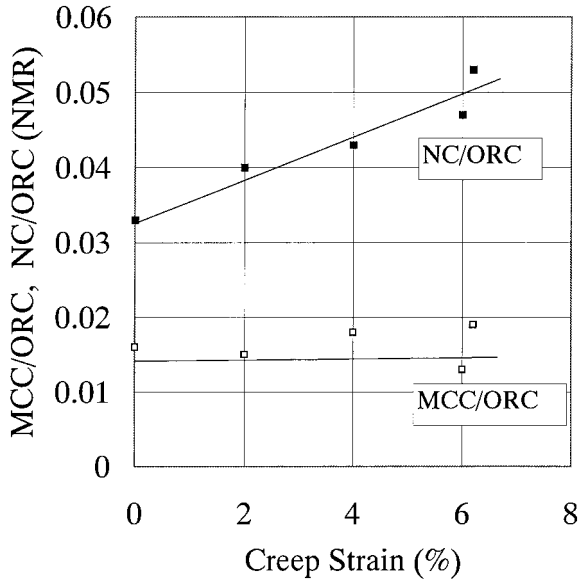

Figure 10 Ratio of the monoclinic phase to the orthorhombic phase (MCC/ORC) and that of the amorphous phase to the orthorhombic phase (NC/ORC) versus the creep strain evaluated by the ^{13}C-NMR technique.

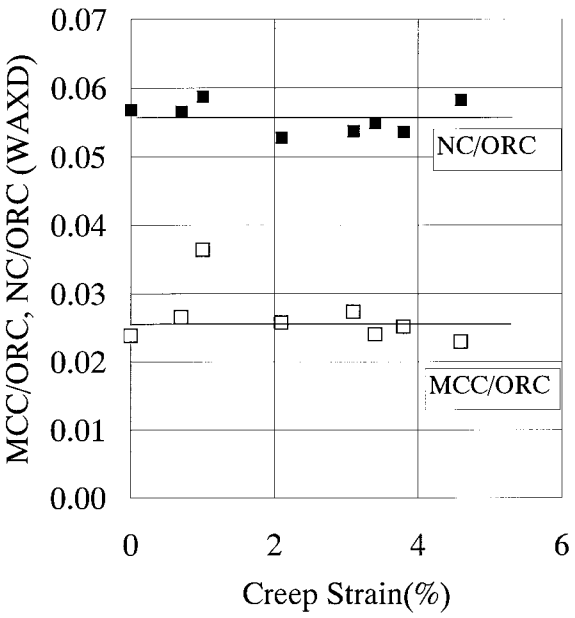

Figure 11 Ratio of the monoclinic phase to the orthorhombic phase (MCC/ORC), and that of the amorphous phase to the orthorhombic phase (NC/ORC) versus the creep strain evaluated by the X-ray technique.

that is needed to support the applied creep stress, then the macroscopic destruction by the propagation of cracks passing through each amorphous area or microvoid occurs at the final stage near the creep rupture. For the first time, the molecular chain breaks should occur at the creep rupture.

Finally, in this study, we cannot explain well about the relationship between the "pseudo-" amorphous region and the results of g_2 value if its trend is significant. Basically, the chain ends or defects are categorized as a first-order defect which has no effect on the Hosemann plot. We assure that this "pseudo-"amorphous phase which exists nearby the crystalline phase may also affect the crystalline lattice as resulted in $g2$-value increase. However, to prove and/or characterize "pseudo-"amorphous region, further precise analysis, for example, the ultra small-angle X-ray scattering method (U-SAXS), should be necessary.

CONCLUSIONS

The structural changes during creep deformation of ultrahigh-strength polyethylene fibers were investigated using several methods. We proposed a new model employing the "pseudo-"amorphous area which increases with the creep deformation up to the creep rupture. This newly generated amorphous area can be detected mainly by the ^{13}C-NMR method but not so clearly with the WAXD method. This contrast is considered to come from the assumption that the originated amorphous area is too small to be detected by WAXD. This suggests that the defects such as chain ends or molecular kinks are excluded from the crystalline area to agglomerate the new amorphous part. This "pseudo-"amorphous area is the derivation of the decrease in the tensile strength and also becomes the direct cause of the creep rupture, where the fiber cannot bear the creep stress.

REFERENCES

1. Smith, P.; Lemstra, P. J.; Kalb, B.; Pennings, A. J. Polym Bull 1979, 1, 733.
2. Smith, P.; Lemstra, P. J. J Mater Sci 1980, 15, 505.
3. Lemstra, P. J.; Kirschbaum, R.; Ohta, T.; Yasuda, H. In Developments in Oriented Polymers-2; Ward, I. M., Ed.; Elsevier: New York, 1987; p 39.
4. Strobl, G.; Ewen, B.; Fischer, E. W.; Piesczek, W. J Chem Phys 1974, 61, 5257.
5. Bonsor, D. H.; Bloor, D. J Mater Sci 1977, 12, 1552.
6. Prevorsek, D. C.; Lyons, W. J. J Appl Phys 1964, 35, 3152.
7. Prevorsek, D. C. J Polym Sci Symp 1971, 32, 343.
8. Coleman, B. D.; Knox, A. G. Text Res J 1957, 27, 393.
9. Papazian, H. A. J Appl Polym Sci 1984, 29, 1547.
10. Trantina, G. G. Polym Eng Sci 1984, 24, 1180.
11. Peterlin, A. J Macromol Sci-Phys B 1981, 19, 401.
12. Sinozaki, D. M.; Howe, R. J Mater Sci 1986, 21, 1735.
13. Grubb, D. T.; Li, Z.-F. Polymer 1992, 33, 2587.
14. Wilding, M. A.; Ward, I. M. Polymer 1978, 19, 969.
15. Wilding, M. A.; Ward, I. M. Polymer 1981, 22, 870.
16. Ward, I. M.; Wilding, M. A. J Polym Sci Polym Phys Ed 1984, 22, 561.
17. Ohta, Y.; Sugiyama, H.; Yasuda, H. J Polym Sci Polym Phys Ed 1994, 32, 261.
18. Ohta, Y.; Yasuda, H. J Polym Sci Polym Phys Ed 1994, 32, 2241.
19. Kaji, A.; Ohta, Y.; Yasuda, H.; Murano, M. Polym J 1990, 22, 455.
20. Egorov, E. A.; Zhizhenkov, V. V.; Marikhin, V. A.; Myasnikova, L. P. J Macromol Sci-Phys B 1990, 29, 129.
21. Scmidt-Rohr, K.; Spies, H. W. Macromolecules 1991, 24, 5288.
22. Tzou, D. L.; Schmidt-Rohr, K.; Spiess, H. W. Polymer 1994, 35, 4728.
23. Bonart, R.; Hosemann, R.; MaCulloughss, R. L. Polymer 1963, 4, 199.
24. Smook, J.; Hamersma, W.; Pennings, A. J. J Mater Sci 1984, 19, 1359.
25. Mark, H. F. In Polymer Science and Materials; Tobolski, A. V.; Mark, H. F., Eds.; Wiley-Interscience: New York, 1971; p 236.
26. Walter, E. R.; Reding, F. P. J Polym Sci 1956, 21, 561.
27. Mansfield, M.; Boyd, R. H. J Polym Sci Polym Phys Ed 1978, 16, 1227.
28. Zhurkov, S. N.; Zakrevskyi, V. E.; Korsukov, V. S.; Kuksenko, A. F. J Polym Sci A2 1972, 10, 1509.
29. Prevorsek, D. C.; Butler, R. H. J Polym Mater 1973, 2, 167.